

CrossMark  
click for updatesCite this: *Anal. Methods*, 2016, 8, 2441

## *In situ* formation of carbon dots aids ampicillin sensing†

Rahul Kumar Mishra,<sup>a</sup> Indra Neel Pulidindi,<sup>a</sup> Eihab Kabha<sup>a</sup> and Aharon Gedanken<sup>\*ab</sup>

A simple analytical method is designed for the detection of micro-molar concentrations of an antibiotic with a  $\beta$ -lactam subunit. The sensor for ampicillin has a limit of detection, LOD, value of  $0.165 \times 10^{-4}$  M and exhibited linearity over a wide range of ampicillin concentrations (6.6–200 ppm). The detection of the antibiotic is based on the *in situ* generation of carbon nanodots (CNDs) via a hydrothermal reaction between glucose and the antibiotic moiety. The CNDs exhibited characteristic absorption at 340 nm whose intensity is a measure of the initial ampicillin concentration. The CNDs possess peculiar blue emission which is excitation independent. The particle size of CNDs is in the range of 8–40 nm and they are hydrophilic in nature. NMR spectral analysis revealed insights into the carbon nano-structure comprising of an aromatic core with carbonyl type functionalities on its surface. Synthesis of carbon dots from ampicillin in aqueous medium and utilizing the absorption properties as well as the emission properties of the carbon dots generated for the detection of ampicillin make the design and operation of the sensor environmentally friendly and simple.

Received 10th February 2016

Accepted 13th February 2016

DOI: 10.1039/c6ay00413j

www.rsc.org/methods

## 1 Introduction

Apart from the major applications in the field of global healthcare, antibiotics provide benefits for agriculture, animal production, and the food industry.<sup>1,2</sup> However, as a consequence of antibiotic abuse, proliferation of resistant species of microorganisms contribute to serious risks to the worldwide public health.<sup>3</sup>  $\beta$ -Lactam antibiotics are the most widely used drugs for veterinary purposes, which lead to the ubiquitous presence of these antibiotics in a variety of animal food products.<sup>4–7</sup> Moreover, the exposure of the environment<sup>8</sup> and water supply<sup>9</sup> to antibiotics generates a worsening situation for the general public, making the detection of  $\beta$ -lactam antibiotics an important issue.

A variety of techniques has been employed for the detection of antibiotics. Among them, the most popular methods are based on liquid chromatography (limit of detection, LOD: 0.5–50  $\mu\text{g kg}^{-1}$ ) and bacterial culture assays (LOD: 2–4  $\mu\text{g kg}^{-1}$ ), which generally require extensive periods of analysis time.<sup>10–12</sup> Recently, an amperometric magneto-biosensor has been reported for sensing ampicillin which takes advantage of penicillin binding proteins (PBPs). But this method is limited to only those  $\beta$ -lactam antibiotics which have very high affinities for both cephalosporins and penicillins. Even though an LOD value

of  $38 \pm 2$  nM is reported for ampicillin, the sensor functioning involves complex biochemical processes.<sup>13</sup> Surface enhanced Raman spectroscopy (SERS) has also been explored for sensing ampicillin. But this method is dependent on the application of silver nanoparticles for the detection of  $\beta$ -lactam antibiotics (LOD: 10 ppb).<sup>14</sup> Therefore, it is still a challenge to develop new methods which are simple, sensitive, cost effective, rapid and able to present direct visual evidence for the detection of  $\beta$ -lactam antibiotics. In this context, carbon nanoparticles (CNPs) have emerged as a promising platform for their fascinating fluorescence properties which emit in the blue-green region.<sup>15,16</sup> Consequently, CNPs have been applied for a variety of sensing applications including nucleic acid,<sup>17</sup> vapors,<sup>18</sup>  $\text{H}_2\text{S}$ ,<sup>19</sup> thrombin,<sup>20</sup> metal ions,<sup>21–24</sup> and glucose.<sup>25</sup> So far, there have been no reports on the exploitation of an antibiotic as a source for generating fluorescent CNPs leading to its quantification. The present report presents a two in one proof of concept that the fluorescent CNPs can be generated *in situ*, during the hydrothermal reaction between ampicillin and glucose, and the newly formed CNPs could be used as a sensor for the quantification of a  $\beta$ -lactam antibiotic.

## 2 Experimental section

Glucose (product no. G8270), ampicillin (product no. A6140), 2-phenyl glycine (product no. P25507), and (+)-6-amino penicillanic acid (product no. A70909) were purchased from Sigma Aldrich and were used as received. Stock solutions of respective compounds were prepared afresh in deionized water. Solutions of desired concentrations were prepared from the stock

<sup>a</sup>Department of Chemistry, Bar-Ilan University, Ramat-Gan 52900, Israel

<sup>b</sup>National Cheng Kung University, Department of Materials Science and Engineering, Tainan 70101, Taiwan. E-mail: gedanken@mail.biu.ac.il

† Electronic supplementary information (ESI) available. See DOI: 10.1039/c6ay00413j

solutions just prior to their use. To generate the carbon dots, the solutions of glucose-ampicillin, ampicillin, 2-phenyl glycine, and (+)-6-amino penicillanic acid were subjected to hydrothermal reaction at 120 °C for 40 min in an autoclave (Tuttnauer Cat 2007). UV-vis spectra of the analytes containing the carbon dots were recorded using a Cary 100 scan varion UV/vis spectrophotometer. Fluorescence emission studies were performed using a fluorescence spectrophotometer (Varian Cary Eclipse) equipped with a 120 W Xenon lamp as the excitation source. Transmission electron microscope images were recorded using a TEM JEOL jem-1400 (120 kV). Powder X-ray diffraction (XRD) was performed with a Bruker D8 Advance X-ray diffractometer using Cu K $\alpha$  radiation operating at 40 kV/40 mA with a 0.0019° step size.  $^1\text{H}$  and  $^{13}\text{C}$  NMR spectra were recorded using a Bruker Avance DPX 300 using D $_2\text{O}$  as a solvent. FT-IR spectra of ampicillin, glucose and carbon dots were recorded on an Avarter model FT-IR spectrometer in the range of 4000–400  $\text{cm}^{-1}$ . Photographs of the aqueous solution of carbon dots were obtained under white light and UV light using a UVL-18 EL series UV lamp (365 nm UV/white/8 watts).

### 3 Results and discussion

A typical assay designed for the determination of ampicillin in the concentration range of  $0.165 \times 10^{-4}$  to  $4.957 \times 10^{-4}$  M (6.6–200 ppm) comprises of taking varying amounts of ampicillin (0.1 wt% solution) and a fixed amount of glucose (5 wt% solution) in water as shown in Table 1.

Table 1 presents the composition of the solutions undergoing the hydrothermal reaction. The aqueous solutions (labelled as H0–H8) were subjected to hydrothermal treatment in an autoclave at 120 °C for 40 min. Subsequently, the solutions were analyzed using electronic spectroscopy. The UV-vis absorption spectra of the solutions after the hydrothermal reaction are shown in (Fig. 1a). It is worth mentioning that a stable colloidal solution is obtained at the end of the hydrothermal reaction without the formation of any precipitate. The presence of ampicillin made a striking difference in the absorption features of the analytes. For instance, in the case of H0 where only glucose (5 wt%) was hydrothermally heated, the solution exhibited two characteristic absorption bands at 225 and 280 nm. Such absorption features could be due to the generation of carbon dots from glucose.<sup>25</sup>

Glucose solution (5 wt%) without hydrothermal treatment did not show any such absorption features. Interestingly, the product solutions (H1–H8) containing varying amounts of ampicillin (0.1–3 mg) exhibited an additional absorption band at 340 nm along with the two bands at 225 and 280 nm.

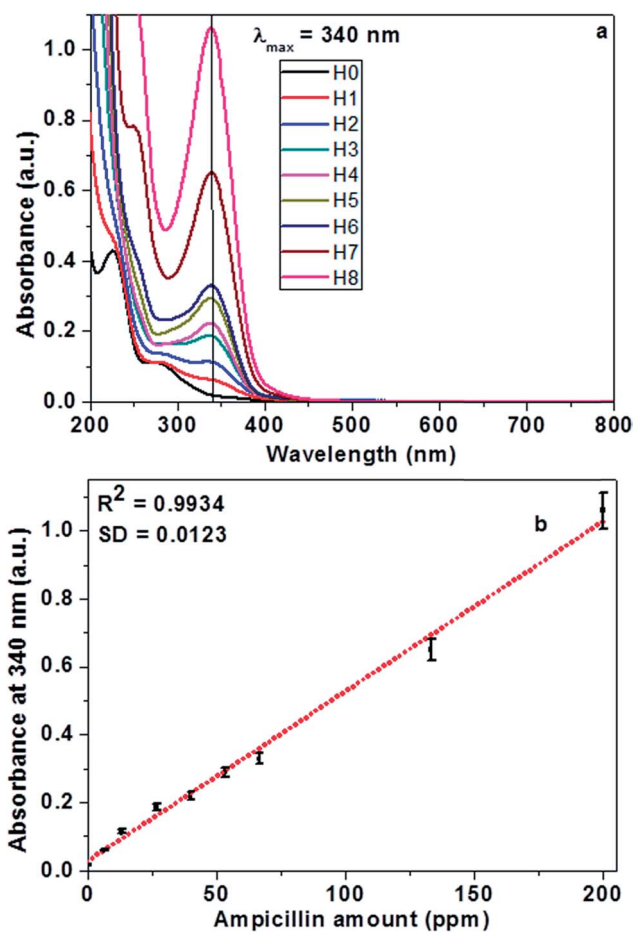


Fig. 1 (a) UV-vis spectra of analytes with different ampicillin amounts (0–200 ppm); (b) calibration plot for ampicillin detection based on the absorption at  $\lambda_{\text{abs}} = 340$  nm of the analytes H0–H8.

Moreover, the intensity of the absorption band at 340 nm increased as a function of the initial ampicillin amount as could be seen in Fig. 1a.

The increase in the absorption intensity of the 340 nm band as a function of ampicillin concentration forms the basis for ampicillin sensing. The intensity of the band at 340 nm in the analytes as a function of ampicillin concentration (from H0–H8) is plotted in Fig. 1b. A linear relationship between these two variables is observed (Fig. 1b). This plot serves as a calibration curve for ampicillin sensing. The calibration plot with a correlation coefficient of 0.9934 ( $R^2$ ) and a standard deviation (SD) value of 0.0123 indicates the accuracy of ampicillin detection. Thus, a sensitive and selective sensor for ampicillin detection is designed.

Table 1 Assay for ampicillin detection in the concentration range of  $0.165 \times 10^{-4}$  to  $4.957 \times 10^{-4}$  M (6.6–200 ppm)

Sample code	H0	H1	H2	H3	H4	H5	H6	H7	H8
Glucose (5%), mL	1	1	1	1	1	1	1	1	1
Ampicillin (0.1%), mL	0	0.1	0.2	0.4	0.6	0.8	1.0	2.0	3.0
Ampicillin (in ppm)	0	6.6	13.3	26.7	40	53.3	66.6	133.3	200
Water, mL	14	13.9	13.8	13.6	13.4	13.2	13	12	11
Total volume, mL	15	15	15	15	15	15	15	15	15

There are few moieties in the ampicillin molecule that could be responsible for the formation of the CND, the first being the poly-aromatic fluorophore.<sup>26,27</sup> Chen *et al.* observed two absorption bands at 246 and 310 nm for the carbon dots generated from polyethylene glycol. They attributed the absorptions to the  $\pi-\pi^*$  transitions of  $-C=C-$  and  $n-\pi^*$  transitions of  $-C=O$  groups, respectively. Moreover, Chen *et al.* attributed the observed red shift in the absorption bands to the formation of larger conjugated structures resulting from longer heating times employed.<sup>28</sup> To probe more deeply into the origin of the two absorption bands (225 and 280 nm) in the case of sample H0, the glucose solution (5 wt%) before and after the hydrothermal treatment was analyzed using NMR ( $^1\text{H}$  and  $^{13}\text{C}$ ) spectroscopy. No perceptible changes either in  $^1\text{H}$  (Fig. S1†) or  $^{13}\text{C}$  (Fig. S2†) spectra of the analytes (glucose 5 wt%) before or after the hydrothermal treatment were observed. Only peaks typical of glucose alone were observed even after the hydrothermal treatment.<sup>29,30</sup> As the hydrothermal reaction conditions are mild (120 °C, 40 min), the concentration of carbon dots generated might be too low to be observed by the NMR spectra.

The origin of the new absorption band at 340 nm could be attributed to the formation of a new energy level in the carbon dot structure due to the reaction between glucose and ampicillin resulting in the incorporation of the heteroatom N into the carbon dot structure. The unique structural advantage of ampicillin possessing an aromatic component as well as heteroatoms (N and S) makes it a promising precursor for the preparation of carbon dots. This is the first report dealing with the use of ampicillin for such applications. Interestingly, the chemical structure of ampicillin comprises of an aromatic ring (phenyl glycine subunit) and the  $\beta$ -lactam ring (amino penicillanic acid subunit) (Scheme S1†). Another unique feature of the ampicillin ( $\text{C}_{16}\text{H}_{19}\text{N}_3\text{O}_4\text{S} \cdot 3\text{H}_2\text{O}$ ) molecule is that, it contains heteroatoms such as N and S. The possible presence of heteroatoms, especially N into the carbon dot structure, could contribute to the formation of additional energy states responsible for the absorption band at 340 nm (Fig. 1a). The formation of a new energy level by the doping of N in the carbon dot structure is shown schematically in Scheme S2.† The absorbance at 340 nm could be attributed to the  $n-\pi^*$  transition of  $\text{C}=\text{N}$ . Zhang *et al.* proposed the formation of a new energy level due to the doping of N in graphene quantum dots.<sup>31</sup> Interestingly Zhang *et al.* detected a similar absorption band ( $\lambda_{\text{abs}} = 342 \text{ nm}$ ) in the case of S and N co-doped carbon dots synthesized from cysteine. Zhang *et al.* have attributed this absorption band to either carbonyl or conjugated carbonyl groups present in the carbon dot structure.<sup>32</sup> Kumar *et al.* detected an absorption band at 350 nm in the absorption spectrum of the N containing model fluorescent molecule quinine sulfate.<sup>33</sup> Carbon dots synthesized from nitrogen containing precursor molecules (citric acid-1,2-ethyl diamine; *N*-(*b*-aminoethyl)-*g*-aminopropyl) exhibited a characteristic absorption at 350 nm.<sup>34</sup> These examples clearly indicate that the origin of the absorption band observed in Fig. 1a is due to the doping of nitrogen in the carbon dot structure formed from the ampicillin molecule.

The presence of glucose along with ampicillin is inevitable for the sensing application of ampicillin *via* the formation of carbon dots. The absorption properties of the carbon dots generated from ampicillin (6–200 ppm) without glucose and with glucose are shown in Fig. S3.† Studies carried out without the presence of glucose but similar ampicillin amounts indicated that even though carbon dots with a typical absorption band at 336 nm could be generated, the increase in the absorption band at 336 nm was not linearly varying as a function of ampicillin concentration (6–200 ppm). Moreover, the sensitivity of ampicillin detection is also enhanced by the presence of glucose. This indicates that the formation of the carbon dot structure comprises of a reaction between glucose and ampicillin.

Tuning of the electronic structure of the carbon nanostructures *via* doping with other elements like N is a well-known strategy that increases the potential application of the generated materials *via* the enhancement of the fluorescence intensity. Dopants like N injects electrons into the carbon structure resulting in the alteration of the electronic properties.<sup>27</sup>

In addition to the characteristic absorbance at 340 nm, the carbon dots generated from the reaction between glucose and ampicillin exhibited blue emission peaked at 427 nm when excited at 340 nm (Fig. 2a).

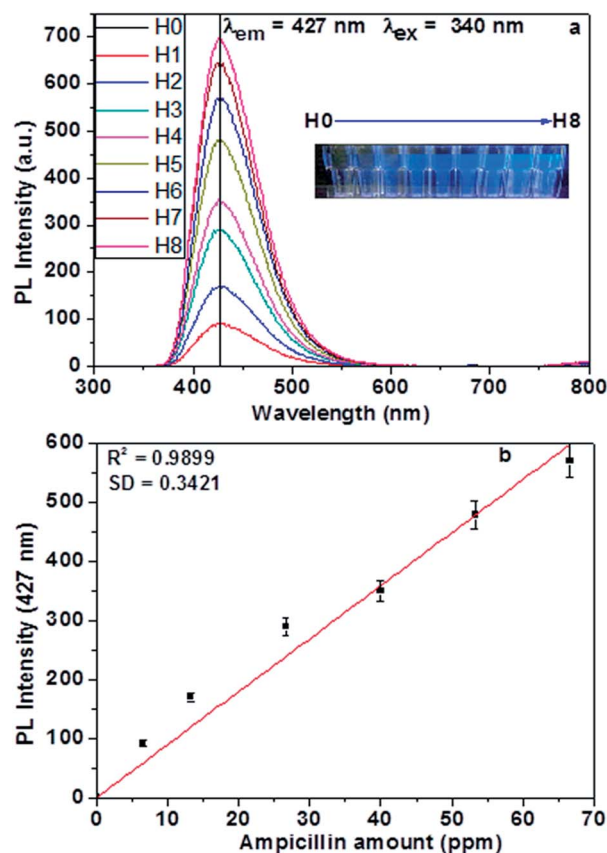


Fig. 2 (a) Photoluminescence spectra (PL) of analytes with different ampicillin amounts (0–200 ppm); (b) calibration plot for ampicillin detection based on the PL emission at  $\lambda_{\text{em}} = 427 \text{ nm}$  ( $\lambda_{\text{ex}} = 340 \text{ nm}$ ) of the analytes H0–H6.

Carbon dots prepared from N-containing precursor molecules like *N*-(*b*-aminoethyl)-*g*-aminopropyl have also exhibited similar emission properties at 450 nm when excited at 360 nm.<sup>34</sup> *L*-isoleucine, *L*-valine and glycine functionalized carbon dots were similar to the carbon dots produced from ampicillin.<sup>35</sup> Zheng *et al.* observed similar absorption and emission features in the carbon dots prepared from citric acid–diethylenetriamine.<sup>36</sup> These results indicate that possible heteroatom (N and S) incorporation into the carbon dot structure formed from ampicillin might be the origin of the emission band at 427 nm. The intensity of the emission at 427 nm is found to vary linearly with the initial ampicillin amount present in the analytes, H0–H6, which could also be used as a measure for ampicillin quantification (Fig. 2).

Moreover, the measured emission was excitation independent with an emission maxima at 427 nm ( $\lambda_{em}$ ) when excited at different wavelengths ( $\lambda_{ex}$  = 280, 300, 320, 360, and 380 nm) as shown in Fig. S4.† Similar excitation independent PL emission characteristics were observed in the carbon dots generated from solution with lower concentrations of glucose (1 wt%) and ampicillin (0.01 wt%) (Fig. S5†).

We hypothesize the presence of heteroatoms (N and S) in the ampicillin molecule to be the major factor contributing the absorption properties, in the region of 300–400 nm, of the carbon dot generated from the glucose–ampicillin reaction upon hydrothermal treatment. To evaluate this hypothesis, two compounds namely, (+)-6-amino penicillanic acid (containing the  $\beta$ -lactam subunit as well as the heteroatoms, N and S) and 2-phenyl glycine were used as precursors for the formation of carbon dots by reacting the respective compounds (0.1 wt%) with glucose (5 wt%) under hydrothermal conditions. The UV-vis absorption spectra of the resulting aqueous solution containing the carbon dots are shown in Fig. 3.

An interesting absorption feature in the region of 300–400 nm which is typical of the sensing application was exhibited by the carbon dots generated from (+)-6-amino penicillanic acid.

On the contrary, 2-phenyl glycine showed an absorption maximum at 260 nm (Fig. 3). Moreover, the color of the aqueous solution of carbon dots generated from the  $\beta$ -lactam ring containing (+)-6-amino penicillanic acid is yellow unlike the carbon dot solution from the 2-phenyl glycine counterpart. The appearance of yellow coloration is a direct visual indication that carbon dot formation is more feasible in the case of (+)-6-amino penicillanic acid rather than 2-phenyl glycine.

In addition, carbon dots generated from (+)-6-amino penicillanic acid exhibited a typical PL emission peak with  $\lambda_{em}$  at 425 nm when excited at 300 nm. On the contrary, under identical excitation conditions, the aqueous solution containing the carbon dots from 2-phenyl glycine did not show any PL emission phenomena (Fig. S6†).

This confirmed our hypothesis that the heteroatom containing the  $\beta$ -lactam subunit in the ampicillin structure is the major factor contributing to the characteristic absorption and emission features of the carbon dots generated in the ampicillin–glucose reaction.

A representative TEM image of the carbon dots with a particle size (diameter) in the range of 8–40 nm generated from the hydrothermal treatment of glucose (5 wt%) – ampicillin (0.01 wt%) solutions is depicted in Fig. 4. The carbon nanoparticles were spherical and well dispersed in an aqueous medium.

The carbon dots viewed in the TEM image authenticate that the sensing of ampicillin is due to the unique absorption properties (at 340 nm) of the carbon dots formed during the hydrothermal reaction between glucose and ampicillin. This is the first ever example for the synthesis of carbon dots from the antibiotics and utilizing the same for the detection and quantification of antibiotics containing the  $\beta$ -lactam subunit.

For gaining further insights into the formation of the carbon nanodot structure through the glucose–ampicillin reaction and also to understand the chemical structure of the carbon dot, systematic NMR spectroscopic studies were carried out.

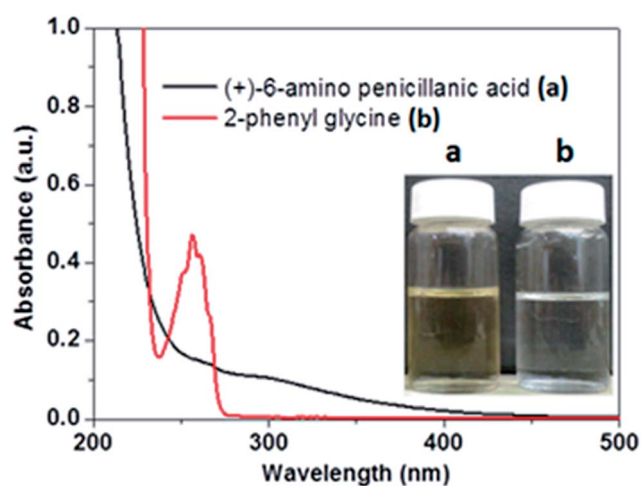


Fig. 3 UV-vis spectra of (a) (+)-6-amino penicillanic acid and (b) 2-phenyl glycine (inset: photographs of an aqueous solution of carbon dots from (a) (+)-6-amino penicillanic acid, (b) 2-phenyl glycine).

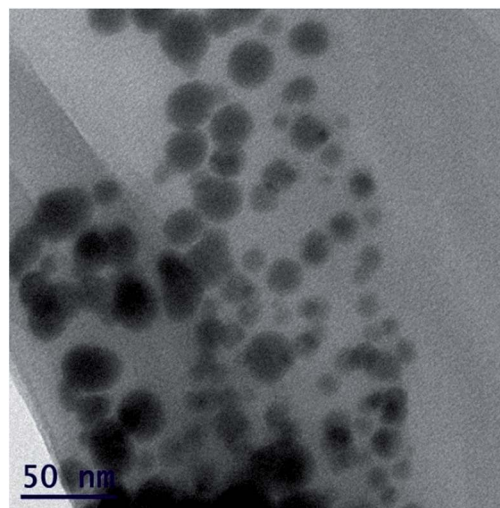


Fig. 4 TEM image of carbon dots generated from glucose (5 wt%) and ampicillin (0.01 wt%) under hydrothermal reaction conditions at 120 °C for 40 min.

$^1\text{H}$  NMR spectra of ampicillin (0.1%, 15 mL) solution before and after the hydrothermal treatment (120 °C, 40 min) are shown in Fig. S7.† The three peaks typical of ampicillin located at 1.46, 3.39 and 7.53 ppm underwent significant changes (peak splitting and broadening) upon hydrothermal treatment. An additional signal at 8.2 ppm was observed indicative of the generation of formate type species ( $\text{HCOO}^-$ ) in the structure. A corresponding peak at 164 ppm in the  $^{13}\text{C}$  NMR spectra of ampicillin solution (0.1 wt%) after hydrothermal treatment confirms the generation of formate type species (Fig. S8†). Aqueous solutions of ampicillin with lower concentrations (533 and 933 ppm) have also been subjected to hydrothermal treatment under identical conditions and analyzed by  $^1\text{H}$  NMR for monitoring the surface functionalities on the carbon dot surface. Interestingly, in the case of the product with 933 ppm ampicillin, the signal characteristic of  $\text{HCOO}^-$  species is observed whereas in the case of the product with 533 ppm ampicillin such a signal is not observed which could be due to the lower concentration of such species being below the detection limit (Fig. S9†). These changes in the spectral features indicate the partial oxidation of ampicillin upon hydrothermal treatment. Similar changes were also observed in the  $^1\text{H}$  (Fig. S10†) and  $^{13}\text{C}$  (Fig. S11†) NMR spectra of the glucose (5 wt%) – ampicillin (0.1 wt%) solution (15 mL, analyte H8, Table 1) upon hydrothermal treatment (120 °C, 40 min). Owing to the milder hydrothermal reaction conditions, even though carbon dots are generated by the reaction of glucose (5 wt%) and ampicillin (0.1 wt%), neither the glucose nor the ampicillin are completely utilized in the carbon dot formation as the peaks typical of both glucose and ampicillin are still observed in the aq. solution of the carbon dots obtained after the hydrothermal reaction. It should be noted that the ampicillin sensing was demonstrated (Fig. 1) based on using the hydrothermal reaction product from the reaction of glucose (5 wt%) – ampicillin (0.1 wt%) without further isolation of carbon dots from the residual glucose. This indicates the ease of the synthesis as well as the application of carbon dots in a single step, avoiding the conventional dialysis process which is usually used for the isolation of carbon dots from the reaction product and is time consuming.

The hydrothermal reaction between glucose (5 wt%) and ampicillin (0.1 wt%), leading to carbon dot formation, was also carried out at higher reaction temperature (150 °C) and for longer duration (2, 4, 6 and 12 h). As a function of reaction time, the peaks typical of ampicillin (0.1 wt%) located at 1.46, 3.39 and 7.53 (Fig. S7†) disappeared and new peaks typical of the carbon dot structure (2.24, 6.68, 7.54 and 9.47 ppm) were evident in the analyte hydrothermally treated for 12 h (Fig. 5d).

The peak at 2.24 ppm corresponds to the protons adjoining the aromatic or  $\text{sp}^2$  protons, the peaks at 6.68 and 7.54 correspond to aromatic or  $\text{sp}^2$  protons and the peak at 9.47 ppm corresponds to the proton bound to the carbonyl group.<sup>28</sup> The carbon nanostructure comprising of the aromatic core with oxygen rich functionalities like  $-\text{C}=\text{O}$  is evident from the NMR spectral analysis (Fig. 5).  $^{13}\text{C}$  NMR spectra of the glucose (5 wt%) – ampicillin (0.1 wt%) solutions subjected to hydrothermal treatment at 150 °C for different time periods (2, 4, 6 and 12 h)

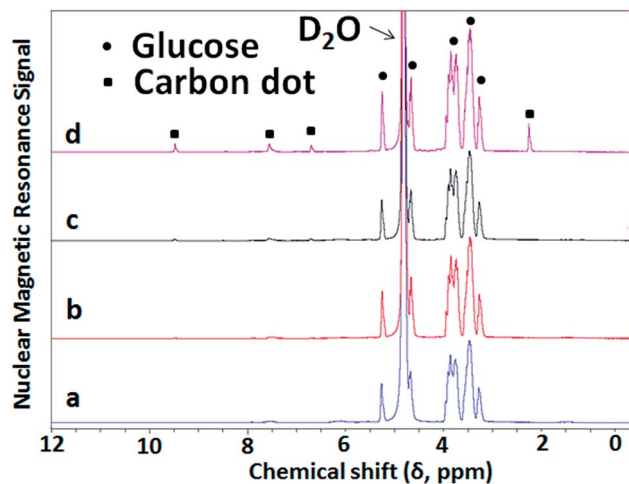


Fig. 5  $^1\text{H}$  NMR spectra of analytes from glucose (5 wt%) and ampicillin (0.1 wt%) solution subjected to hydrothermal treatment at 150 °C for (a) 2 h, (b) 4 h, (c) 6 h and (d) 12 h.

are shown in Fig. S12.† New signals characteristic of the carbon dot structure could be observed at 31.1, 56.8, 111.9, 152.7, 162.2, 181.4 and 216.1 ppm at the expense of ampicillin peaks. In addition, peaks typical of glucose (60–100 ppm) were also observed as glucose was taken in excess (5 wt%) and not all glucose is utilized for the formation of carbon nanodots. The surface functional groups on the carbon dots were further analyzed using FT-IR spectroscopy. A typical FT-IR spectrum of ampicillin showed consecutive intense signals in the range of 950–1750  $\text{cm}^{-1}$ . The strong bands at 1647 and 1740  $\text{cm}^{-1}$  were attributed to the carboxyl group and the carbonyl group of the four membered ring of the ampicillin molecule. In addition, two bands of medium intensity typical of the heterocyclic S–C stretching vibration at 640 and 696  $\text{cm}^{-1}$  were observed (Fig. S13†).<sup>37,38</sup> A representative FT-IR spectrum of the carbon nanodot (CND) solution obtained after a hydrothermal reaction at 150 °C for 12 h is shown in Fig. S14(a).† Characteristic bands of ampicillin in the range of 1000–2000  $\text{cm}^{-1}$  were absent in the CND solution indicating complete conversion of ampicillin to carbon dots. As the glucose amount was taken in excess (5 wt%), the unreacted glucose could also be observed in the FT-IR spectrum of the CND solution (Fig. S14a†). Interestingly, new bands typical of the carbon dot structure could be seen at 1463 and 1662  $\text{cm}^{-1}$  which could be attributed to the ring C=C stretching vibration and the carboxyl functional groups, respectively. This observation is consistent with the  $^1\text{H}$  NMR analysis (Fig. 5d). Thus, the aromatic carbon structure forms the core of the carbon nanodot structure with carboxyl type surface functional groups. A typical FT-IR spectrum of aq. glucose (5 wt%) is shown in Fig. S14(b)† with characteristic bands in the range of 1000–1500 and 2900–3600  $\text{cm}^{-1}$ .<sup>39</sup> The carbon dot–glucose composite was isolated from the aq. glucose (5 wt%) – ampicillin (0.1 wt%) solutions subjected to hydrothermal treatment at 150 °C for 2, 4, 6 and 12 h *via* rotoevaporation and analyzed by XRD (Fig. S15†). Two broad diffraction peaks in the range of 10–30 and 40–50° were observed in the carbon dot–glucose composites. These two peaks were typical of amorphous

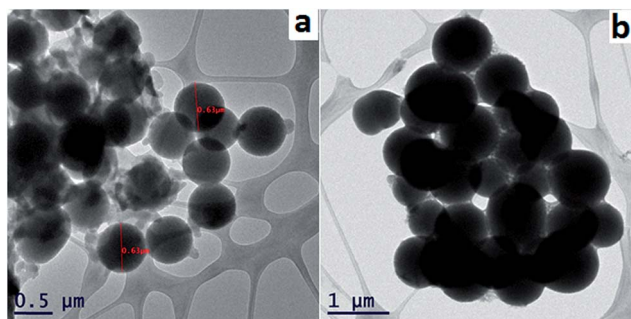


Fig. 6 TEM images of carbon particles produced from glucose (5 wt%) and ampicillin (0.1 wt%) solution subjected to hydrothermal treatment at 150 °C for (a) 4 h and (b) 12 h.

carbon materials. A similar diffraction pattern was exhibited by carbon quantum dots with turbostratic disorder synthesized from citric acid with branched polyethyleneimine.<sup>40</sup>

With an increase in the hydrothermal reaction time, the intensity of the afore mentioned peaks steadily decreased indicative of the increased amorphous nature and extensive conjugated aromatic carbon structure. Such a phenomenon is further substantiated from the TEM images of the carbon particles obtained from the hydrothermal reaction of glucose (5 wt%) and ampicillin (0.1%) for a longer time (2–12 h).

Typical TEM images of spherical carbon particles produced after 4 and 12 h of a hydrothermal reaction having particle sizes of 0.63 μm and 0.88 μm, respectively are shown in Fig. 6. Thus the particle size of carbon dots substantially increased from <40 nm to ~880 nm as the hydrothermal reaction conditions are varied from 40 min at 120 °C to 12 h at 150 °C.

Even though the current report dealing with the development of a chemical sensor for ampicillin detection based on the reaction between ampicillin and glucose under modest hydrothermal reaction conditions (120 °C, 40 min) is innovative, there is further scope for improvement in the performance of the sensor for real applications and evaluating the effect of interference on the selectivity of the sensor. Such studies are in progress. Owing to the characteristic excitation independent blue emission of the carbon dots generated from ampicillin they could find applications in diverse areas like bioimaging and heavy metal ion sensing.

## 4 Conclusions

Herein, we present for the first time, a validation for the two in one proof of concept that a β-lactam antibiotic can be exploited as a scaffold for the generation of fluorescent carbon nanoparticles (CNPs) and consequently as an effective platform for the detection of the β-lactam containing antibiotic species. This concept was demonstrated with the specific example of using an unconventional organic precursor, ampicillin, for the generation of water soluble CNPs with peculiar absorption and emission properties. The CNPs exhibited a characteristic absorption at 340 nm which varied linearly with increasing ampicillin concentration. This characteristic absorption band formed the

basis for sensing ampicillin in a given analyte with accuracy down to 0.6 ppm. Moreover, the CNPs exhibited characteristic excitation independent blue emission. The β-lactam ring is found to be imperative for the formation of CNDs which was demonstrated in the specific case of (+)-6-amino penicillanic acid. This makes the current methodology applicable for the detection of other antibiotics containing the β-lactam ring.

## Notes and references

- 1 L. M. Durso and K. L. Cook, *Curr. Opin. Microbiol.*, 2014, **19**, 37.
- 2 R. S. Singer and J. Williams-Nguyen, *Curr. Opin. Microbiol.*, 2014, **19**, 1.
- 3 L. Rizzello and P. P. Pompa, *Chem. Soc. Rev.*, 2014, **43**, 1501.
- 4 G. Suarez, Y. H. Jin, J. Auerswald, S. Berchtold, H. F. Knapp, J. M. Diserens, Y. Leterrier, J. A. E. Manson and G. Voirin, *Lab Chip*, 2009, **9**, 1625.
- 5 H. Oka, Y. Ikai, Y. Ito, J. Hayakawa, K. Harada, M. Suzuki, H. Odani and K. Maed, *J. Chromatogr., B: Anal. Technol. Biomed. Life Sci.*, 1997, **693**, 337.
- 6 F. C. Cabello, *Environ. Microbiol.*, 2006, **8**, 1137.
- 7 J. J. Dibner and J. D. Richards, *Poult. Sci.*, 2005, **84**, 634.
- 8 X. Pan, Z. Qiang, W. Ben and M. Chen, *Chemosphere*, 2011, **5**, 695.
- 9 W. Giger, A. Alder, E. M. Golet, H. P. E. Kohler, C. McArdell, E. Molnar, H. Siegrist and M. J. F. Suter, *Chimia*, 2003, **57**, 485.
- 10 A. A. M. Stolker and U. A. T. Brinkman, *Chromatographia*, 2005, **1067**, 15.
- 11 L. Kantiani, M. Farre and D. Barcelo, *Anal. Chem.*, 2009, **28**, 729.
- 12 M. H. Le Breton, M. C. Savoy-Perroud and J. M. Diserens, *Anal. Chim. Acta*, 2007, **586**, 280.
- 13 M. Gamella, S. Campuzano, F. Conzuelo, M. Esteban-Torres, B. de las Rivas, A. J. Reviejo, R. Munoz and J. M. Pingarron, *Analyst*, 2013, **138**, 2013.
- 14 C. Andreou, R. Mirsafavi, M. Moskovitsa and C. D. Meinhart, *Analyst*, 2015, **140**, 5003.
- 15 J. Zhang, W. Shen, D. Pan, Z. Zhang, Y. Fang and M. Wu, *New J. Chem.*, 2010, **34**, 591.
- 16 H. K. Sadhanala, J. Khatel and K. K. Nanda, *RSC Adv.*, 2014, **22**, 11481.
- 17 H. Li, Y. Zhang, L. Wang, J. Tiana and X. Sun, *Chem. Commun.*, 2011, **47**, 961.
- 18 D. Kim, P. V. Pikhitsa, H. Yang and M. Choi, *Nanotechnology*, 2011, **22**, 485501.
- 19 C. Yu, X. Li, F. Zheng, F. Zheng and S. Wu, *Chem. Commun.*, 2013, **49**, 403.
- 20 Y. Wang, L. Bao, Z. Liu and D. W. Pang, *Anal. Chem.*, 2011, **83**, 8130.
- 21 H. Li, J. Zhai and X. Sun, *Langmuir*, 2011, **27**, 4305.
- 22 M. Algarra, B. B. Campos, K. Radotic, D. Mutavdzic, T. Badosz, J. Jimenez-Jimenez, E. Rodriguez-Castellon and J. C. G. Esteves da Silva, *J. Mater. Chem. A*, 2014, **2**, 8342.

- 23 M. Lan, J. Zhang, Y. S. Chui, P. Wang, X. Chen, C. S. Lee, H. L. Kwong and W. Zh, *ACS Appl. Mater. Interfaces*, 2014, **6**, 21270.
- 24 W. Lu, X. Qin, S. Liu, G. Chang, Y. Zhang, Y. Luo, A. M. Asiri, A. O. Al-Youbi and X. Sun, *Anal. Chem.*, 2012, **84**, 5351.
- 25 I. N. Pulidindi and A. Gedanken, *Int. J. Environ. Anal. Chem.*, 2014, **94**, 28.
- 26 H. Li, X. He, Y. Liu, H. Huang, S. Lian, S. T. Lee and Z. Kang, *Carbon*, 2011, **49**, 605.
- 27 Z. Ma, H. Ming, H. Huang, Y. Liu and Z. Kang, *New J. Chem.*, 2012, **36**, 861.
- 28 M. Chen, W. Wang and X. Wu, *J. Mater. Chem. B*, 2014, **2**, 3937.
- 29 I. N. Pulidindi, B. B. Kimchi and A. Gedanken, *Renewable Energy*, 2014, **71**, 77.
- 30 L. Korzen, I. N. Pulidindi, A. Israel, A. Abelson and A. Gedanken, *RSC Adv.*, 2015, **5**, 16223.
- 31 B. X. Zhang, H. Gao and X. L. Li, *New J. Chem.*, 2014, **38**, 4621.
- 32 Y. Zhang and J. He, *Phys. Chem. Chem. Phys.*, 2015, **17**, 20154.
- 33 V. B. Kumar, Z. Porat and A. Gedanken, *Ultrason. Sonochem.*, 2016, **28**, 367.
- 34 S. Y. Lim, W. Shen and Z. Gao, *Chem. Soc. Rev.*, 2015, **44**, 362.
- 35 S. Sarkar, K. Das, M. Ghosh and P. K. Das, *RSC Adv.*, 2015, **5**, 65913.
- 36 M. Zheng, Z. Xie, D. Qu, D. Li, P. Du, J. Xiabin and S. Sun, *ACS Appl. Mater. Interfaces*, 2013, **5**, 13242.
- 37 S. Gunasekaran, S. R. Varadhan and N. Karunanidhi, *Proc. Indian Natl. Sci. Acad., Part A*, 1996, **62**, 309.
- 38 E. G. Totoli and H. R. N. Salgado, *Phys. Chem.*, 2012, **2**, 103.
- 39 M. Ibrahim, M. Alaam, H. El-Haes, A. F. Jalbout and A. D. Leon, *Eclética Química*, 2006, **31**, 15.
- 40 Y. Dong, R. Wang, H. Li, J. Shao, Y. Chi, X. Lin and G. Chen, *Carbon*, 2012, **50**, 2810.